

Electron Crystallography in Surface Structure Analysis

C. LESLIE, E. LANDREE, C. COLLAZO-DAVILA, E. BENGU, D. GROZEA, AND L. D. MARKS*

Materials Science and Engineering, Northwestern University, Evanston, Illinois 60208

KEY WORDS low energy electron diffraction (LEED); reflection high energy electron diffraction (RHEED); photoelectron holography (PEH); transmission electron microscopy (TEM); transmission electron diffraction (TED); direct methods; Maximum Entropy; Minimum Relative Entropy; surface structure

ABSTRACT Surface structure analysis is an important area of research, and in recent years notable advances have been made in this field, both in improved techniques for studying surfaces and in methods of analyzing them. This review aims to summarize the techniques available, particularly those relating to electron microscopy, and also to outline one of the newest areas of development, the application of direct methods to surface structure analysis. *Microsc. Res. Tech.* 46:160-177, 1999. © 1999 Wiley-Liss, Inc.

INTRODUCTION

It has been known for many years that the chemical and physical properties of a material are dependent on the crystal structure of the compound (Barker and Auerbach, 1984; Hudson, 1992; Zangwill, 1988). The development of direct methods of phasing for X-ray (Hauptman and Karle, 1953; Woolfson and Fan, 1995) and electron diffraction (Dorset, 1995; Vainshtein, 1964) analysis have made crystallography a flourishing field in science. The use of direct methods in surface structure analysis has, however, only begun to develop recently (Landree et al., 1997; Marks and Landree, 1997; Marks et al., 1997). This review aims to summarize the progress made in this field.

A surface acts as an interface between two phases, and this interface may exhibit properties which control the behavior of the system. These properties are a direct result of the surface structure, and, in order to design systems that utilize these fully, the surface structure should be known (Somorjai and Starke, 1992; Venables et al., 1984). A surface structure is not, however, easy to predict. While it may share some characteristics with that of the bulk, the atomic positions are much more influenced by the external environment. If the bulk crystal structure arrangement simply stops at the surface, the atoms are left with fewer neighbors, and therefore a high-energy, low-stability system is formed. In general, this leads to some form of reorganization, where the atoms rearrange themselves to positions of lower energy. Such realignment of atoms to energetically favorable positions can extend for several layers into the bulk, and this too must be correctly identified if the properties of the material are to be fully understood.

Despite rearranging to the lowest energy state possible, the atoms on a surface are still of relatively high energy, and thus more likely to react with other species. The rate at which a monolayer of a species covers a surface is pressure-dependent (Somorjai, 1995); for a material with a sticking coefficient of unity, a monolayer will be deposited in approximately 3 seconds at a pressure of 10^{-6} torr. If the pressure is reduced to 10^{-9} torr however, the deposition time rises to around an

hour (Pruyton, 1994). Thus, in order to study "clean" surfaces, Ultra High Vacuum (UHV) systems, capable of 10^{-10} torr or better, must be used. These were developed in the 1960s, and the development of techniques to study surfaces has run in parallel with improvement of these systems. In recent years UHV systems that have transmission electron microscope facilities attached have been developed, and this has opened up a new area of surface investigation (Bonevich and Marks, 1992; Collazo-Davila et al., 1995; Jayaram et al., 1995; Takayanagi et al., 1978).

The quality of the sample is of the utmost importance in such studies. In general, the specimen is first treated by some combination of dimpling and mechanical lapping or polishing to create regions that will be suitable for electron beam studies. Once this is achieved, the sample is placed in a UHV system, where it undergoes further cleaning, usually by a combination of ion beam bombardment and annealing, until a reproducible clean surface is obtained. This method of preparation generally works well, although in some cases the ions induce specimen damage, which is difficult to overcome (Dunn et al., 1991; Marks et al., 1991). It is important to monitor the sample surface during the experimental procedure, since even at low pressures residual gases are present that may react with the surface. Monitoring is most commonly achieved using Auger electron spectroscopy (AES) to track the chemical composition of the surface (Weissman and Müller, 1981).

Many techniques now exist for studying surfaces, although quantitative analysis of the actual surface structure is still a very specialized field. Scanning tunneling microscopy (STM) can show where areas of electron density lie at the surface (see, for example, van de Leemput and van Kempen, 1992), but identifying atomic type is difficult (Spence et al., 1996), and it does

Contract grant sponsor: National Science Foundation; Contract grant number: DMR-9214505.

*Correspondence to: L. D. Marks, Catalysis Center, Materials Science and Engineering, Northwestern University, 2145 Sheridan Road, Evanston, IL 60208. E-mail: Idm@apollo.numis.nwu.edu

Received 23 December 1997; accepted in revised form 7 April 1998

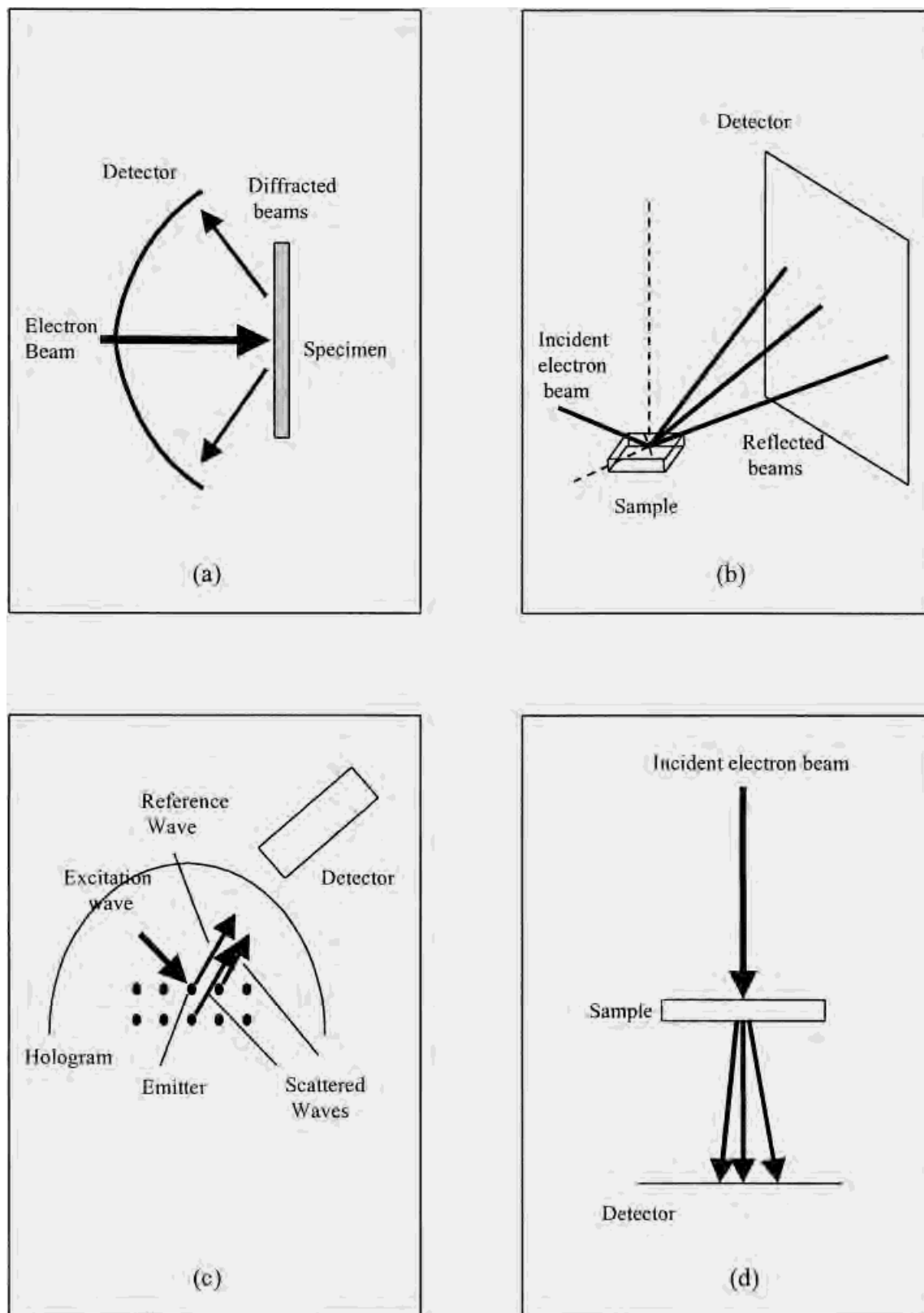


Fig. 1. Comparison of various surface structure analysis experimental techniques. **a:** Low energy electron diffraction (LEED). **b:** Reflection high energy electron diffraction (RHEED). **c:** Photoelectron holography (PEH). **d:** Transmission electron diffraction (TED).

not assist in the identification of subsurface rearrangements. Techniques such as AES (Turner and Schreifels, 1994; Mroz, 1996), X-ray photoelectron spectroscopy (XPS) (Grimblot et al., 1990; Turner and Schreifels, 1994), secondary ion mass spectrometry (SIMS) (Greenlief and White, 1993), and Rutherford backscattering (RBS) (Chu and Liu, 1996) give information about the chemical composition and chemical configuration of the atoms at the surface. These techniques do not give any detail as to the atomic positions, nor do they provide any information about the layers below the surface, which could prove important. To obtain information about atomic positions on the surface and the surface substructure, diffraction techniques must be utilized. The results from analysis of diffraction data from a surface may be used directly or combined with the results from the techniques already mentioned to solve the surface structure. Both X-ray (Feidenhans'l, 1989; Robinson and Tweet, 1992) and electron diffraction (Jayaram et al., 1993, 1995; Takayanagi et al., 1985b) techniques can be used, but for the purposes of this review only experimental electron diffraction techniques will be mentioned in any detail.

EXPERIMENTAL METHODS

Low Energy Electron Diffraction (LEED)

LEED analysis has been widely used as a tool in surface structure analysis for many years (Heinz, 1988, 1995; Jona et al., 1982; Van Hove, 1997). Electrons of approximately 20–500eV energy are easily scattered by atoms, but if they penetrate into a solid by more than approximately six atomic layers, they are adsorbed. If, however, they are back-scattered out of the sample, these electrons will provide information about the atomic positions, symmetry, and, in many cases, periodicity of the structure concerned.

The experimental procedure is relatively straightforward (see Fig. 1a). An electron gun produces a monochromatic electron beam, incident on the specimen, and a detector measures the diffracted beams. Both sharp spot (LEED) and diffuse (DLEED) electron-diffraction patterns may be obtained, where the type of pattern is dependent on the surface order present. Structure analysis is possible from both types of patterns. In order to obtain information about the atomic positions, the intensities of the diffracted beams must be considered. This is not straightforward, since simple kinematic scattering theory is not sufficient, and dynamical models are required. For LEED, dynamical scattering theory (Pendry, 1974, 1994; Tong, 1994) is used to obtain plots of the intensity of a beam against its energy on an I-V curve, and structural analysis is then achieved by comparing the experimental results to those plots. DLEED analysis has developed relatively recently (Heinz, 1994, 1995; Pendry and Saldin, 1984), and follows the same procedure as that for LEED. An advantage of DLEED is that it can also be used to produce two-dimensional intensity maps, which may be used as electron holograms (Saldin and De Andres, 1990) to reproduce the surface structure directly. This does not work for single energy analysis (Wei and Tong, 1992), however, and large data sets are required in order to produce comprehensible results, limiting the usefulness of this technique.

TABLE 1. Surface Structures That Have Been Studied Using the MRE Method

Structure	Data	Reference
Si(111)-(3 × 3) R30° Au	Electron	Marks et al. (1997)
Si(111)-(5 × 2) Au	Electron	Marks et al. (1997)
Si(111)-(7 × 7)	Electron	Gilmore et al. (1997)
Si(111)-(4 × 1) In	Electron	Collazo-Davila et al. (1997)
Si(111)-(6 × 6) Au	X-ray	Marks et al. (1998a)
TiO ₂ (100)-1 × 3	X-ray	Landree et al. (1998) Collazo-Davila et al., (1998b)
Si(111)-(3 × 1) Ag	Electron	Grozea et al. (1999)
Si(111)-(3 × 3) R30° Ag	Electron	Collazo-Davila et al. (1998a)
Ge(111)-(4 × 4) Ag	X-ray	Plass et al. (1998)
MgO(111)-(3 × 3) R30°	Electron	Plass et al. (1998)
MgO(111)-(2 × 2)	Electron	Plass et al. (1998)
MgO(111)-(2,3 × 2,3) R30°	Electron	Plass et al. (1998)
Ni(111)-(5,2 × 2) S	X-ray	Marks et al. (1998b)
Cu(111)- $\begin{vmatrix} 4 & 1 \\ -1 & 4 \end{vmatrix}$ S	X-ray	Marks et al. (1998b)
Cu(110)-p(4 × 1) Bi	X-ray	Marks et al. (1998b)

The main drawback to LEED analysis is that it is a “trial and error” method, in which models are proposed and compared to the experimental data until a fit between the two is found. Advances have been made in recent years in the reduction of time involved in calculating intensities (tensor LEED) (Rous, 1992; Rous and Pendry, 1989a,b; Rous et al., 1986), and the development of directed search methods to improve the starting models (linear LEED) (Rous et al., 1990; Wander et al., 1992). While this has improved the timescale of an analysis, the fact remains that a poor initial model structure will make a LEED analysis particularly complex.

Reflection High Energy Electron Diffraction (RHEED)

In the RHEED technique, a high energy electron beam of energy approximately 3–100 keV is angled towards the specimen surface. The electrons are diffracted by the sample surface, and picked up by a recording device positioned opposite the source (see Fig. 1b). The diffraction pattern consists of a series of streaks, with the sharpness of each streak related to the roughness of the surface on the atomic scale (Ichimiya et al., 1997; Korte and Meyerehmsen, 1993; Ma and Marks, 1990; Maksym, 1985). As with LEED, dynamical scattering theory must be applied in order to understand the diffraction pattern fully (Ichimiya et al., 1993; Ma and Marks, 1992; Maksym and Beeby, 1981; Peng and Cowley, 1986; Peng et al., 1996). Plotting the intensity of the diffracted beams against the angle of incidence gives a rocking curve, and these curves may be used to analyze atomic positions, since the intensity of a diffracted beam is a function of the three-dimensional structure (Nakahara and Ichimiya, 1991; Hashizume et al., 1994). Azimuthal plots and analysis of the intensity distribution in a RHEED pattern are also used in structure determination (Mitura and Maksym, 1993; Hashizume et al., 1995).

The technique is not without problems (Price, 1992). The diffraction pattern obtained is a projection of the reciprocal lattice, and so the sample must be rotated to give information about a second projection. This can prove difficult. Interpretation of the data is not straight-

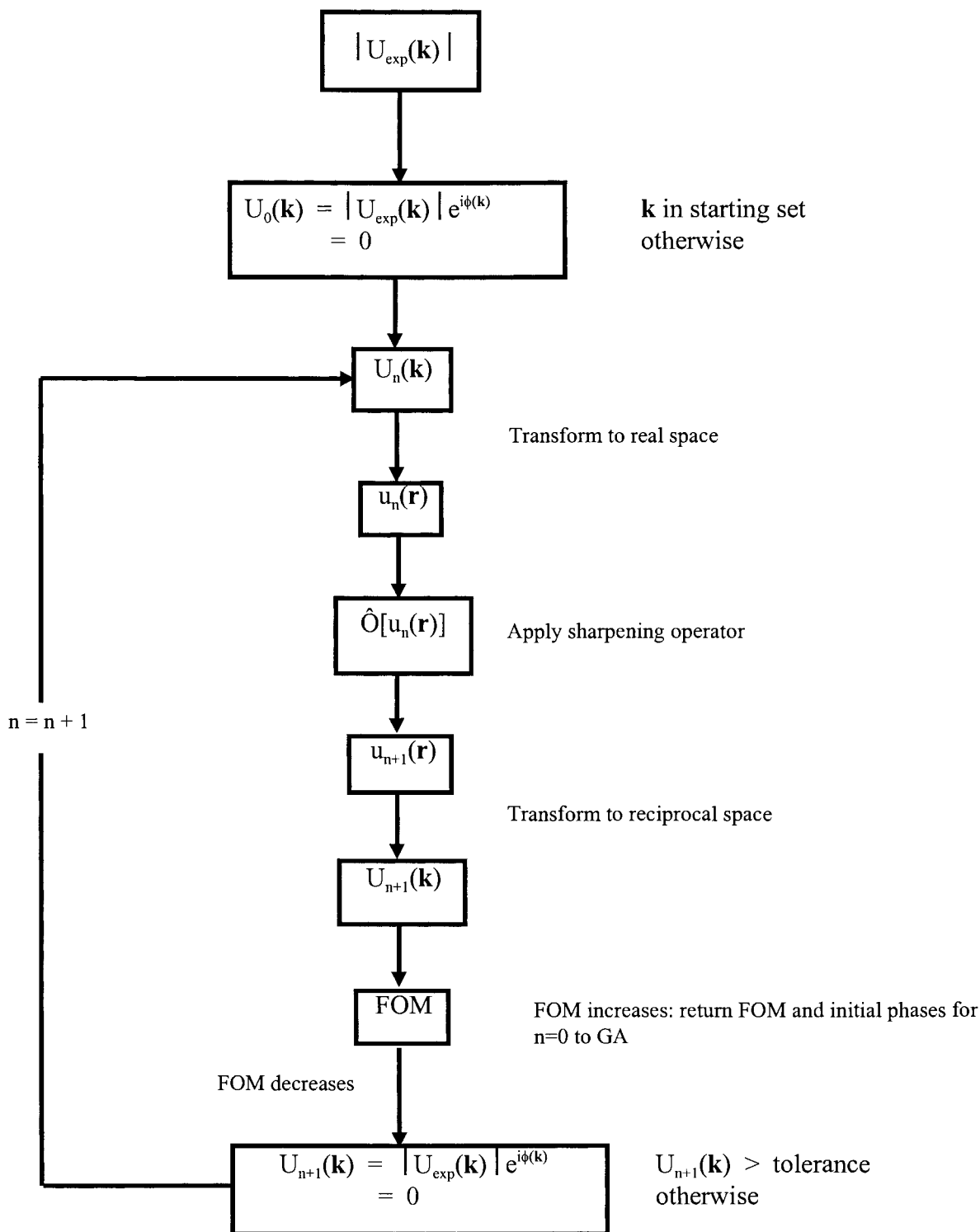


Fig. 2. Flow chart illustrating MRE calculation.

forward, and information can be lost from the diffraction pattern due to incorrect analysis of the streaks. Thus, while RHEED is capable of structural analysis (Ichimiya et al., 1997), it is a fairly complicated and time-consuming method, which in practice is used

more as a monitor of surface roughness, for example in molecular beam epitaxy (MBE) studies (Price, 1992), or to monitor the level of contamination on a surface, though AES is more commonly used for this purpose.

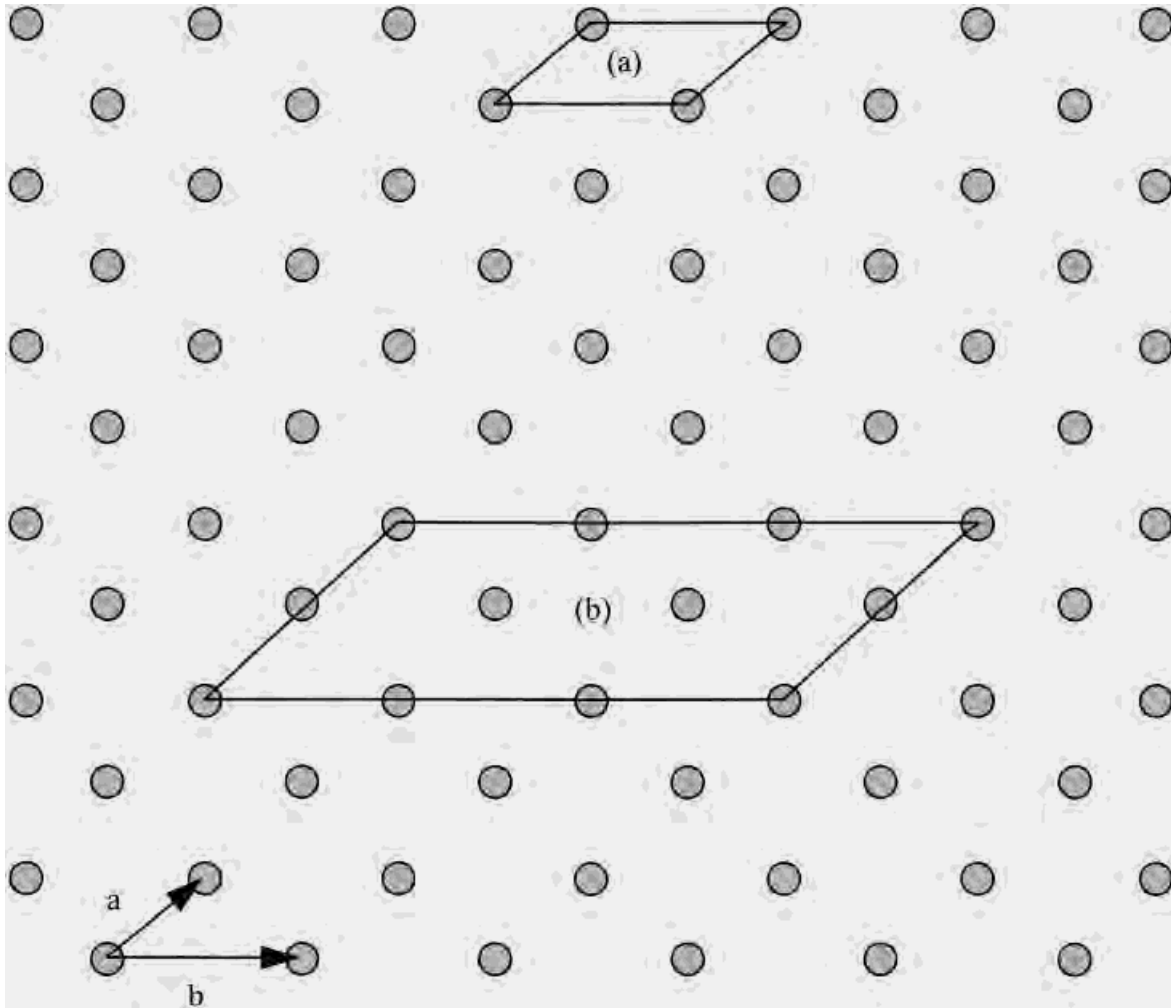


Fig. 3. Illustration of surface notation. Lattice is representative of (111) face of a face-centered cubic structure, with (a) a (111)-(1 × 1) unit cell and (b) a (111)-(2 × 3) unit cell marked.

Photoelectron Holography (PEH)

A photoelectron hologram is a two-angle photoelectron diffraction pattern that can be reconstructed to create a three-dimensional image of the structure of a solid surface from which the diffraction data were obtained (Szöke, 1986). The source of the coherent electrons is a group of atoms located inside the target object (see Fig. 1c). An atom absorbs a photon and produces a photoelectron as the reference wave. The object is assumed to scatter these coherent electrons only weakly, and thus the incident reference-wave amplitude is largely unaffected by passing through the object. The limited interaction between the reference wave and the object produces scattered waves, however, and these interfere with the reference wave to produce the diffraction pattern or hologram. This may then be Fourier transformed to produce an atomic image of the local surface area (Barton, 1990; Fadley et al., 1997; Len et al., 1995; Reuter et al., 1997; Saldin, 1997).

PEH is a relatively new technique, and as such it is difficult to comment on its effectiveness. So far for the systems it has been used to study, it has proved to be an

extremely useful tool, although these systems have not, as yet, been particularly complex. In terms of experimental requirements, PEH is perhaps one of the more user-friendly surface analysis methods, and it may prove to be a popular and reliable technique for determining surface structures in the future.

Transmission Electron Microscopy (TEM) and Diffraction (TED)

The previously discussed techniques are limited to studying the first few layers of a specimen. While this is advantageous in many ways, it does mean that bulk interactions with the surface are not accessible. TEM and TED studies, like X-ray diffraction analysis, allow bulk and surface structures to be considered at the same time (see Fig. 1d).

Images obtained from TEM studies provide useful structural information (Cowley, 1986; Gibson et al., 1997; Williams and Marks, 1995). Profile imaging (Ikarashi et al., 1988; Marks, 1983, 1984; Marks and Smith, 1983), in which the incident beam is parallel to the surface of interest, produces images that show

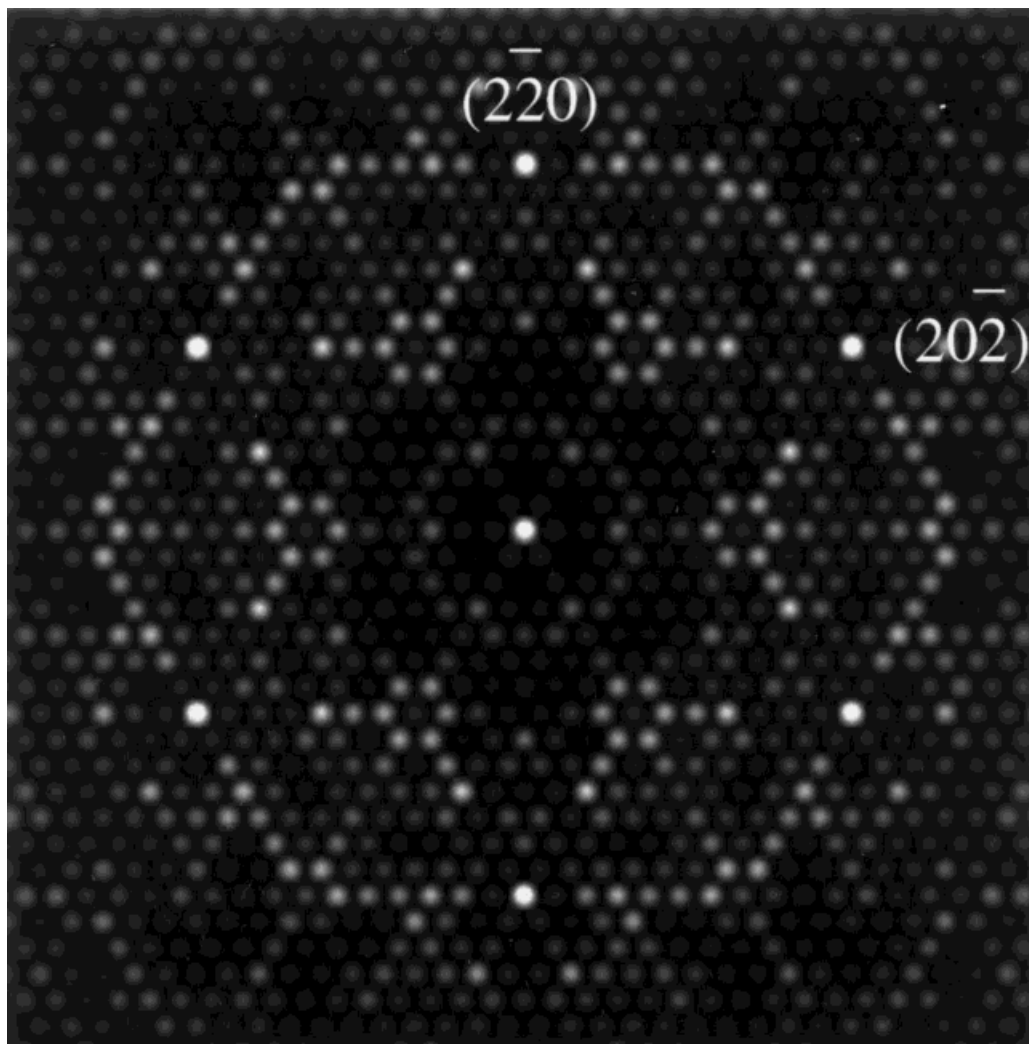


Fig. 4. Restored TED pattern from a Si-(111)-(7 × 7) surface. Experimental intensities from the Si-(111)-(7 × 7) surface were used, with the bulk spots interpolated from these. Bulk spots are indexed.

atomic positions on the surface, but it is difficult to obtain reproducible results, due to the thermodynamic instability of a thin edge. Plan view imaging, in which the incident beam is perpendicular to the surface, can be used either on or off a zone axis, and can provide images that give important phase information, as well as atomic-scale structural information (Dunn et al., 1991; Marks, 1992b; Marks et al., 1992, 1993; Nihoul et al., 1984).

Collection of TED data is a relatively straightforward process, and is usually carried out via a series of exposures on photographic film, CCD or image plate recording. TED patterns yield the intensities of the diffraction spots, as well as partial information about the unit cell symmetry and dimensions (Jayaram et al., 1993; Marks, 1992a; Xu and Marks, 1992a,b), but the intensity data must be reduced to overcome both the problems of diffuse scattering in a diffraction pattern and the low signal-noise ratio of surface diffraction spots. This is done by means of cross-correlation (Xu et al., 1994). Unlike LEED and RHEED, surface electron

diffraction may be assumed to be approximately kinematical, providing the sample is tilted off-zone, (Tanishiro and Takayanagi, 1989; Twosten and Gibson, 1994), and therefore much more straightforward to analyze. It should be noted that the diffraction patterns obtained are two dimensional, meaning that only atomic movement in the plane of the surface can be assessed directly from one diffraction pattern. This can lead to difficulties, for example, in deciding whether one atom sits above or below another.

As with the other methods discussed, this work must be carried out in UHV. As with other forms of microscopy, there is a possibility that the electron beam will cause radiation damage to the specimen, and, in this case, may also provide sufficient energy for surface rearrangements to occur.

ANALYTICAL METHODS Current Techniques

The techniques outlined above provide the raw data for surface structure analysis. In the case of LEED, this

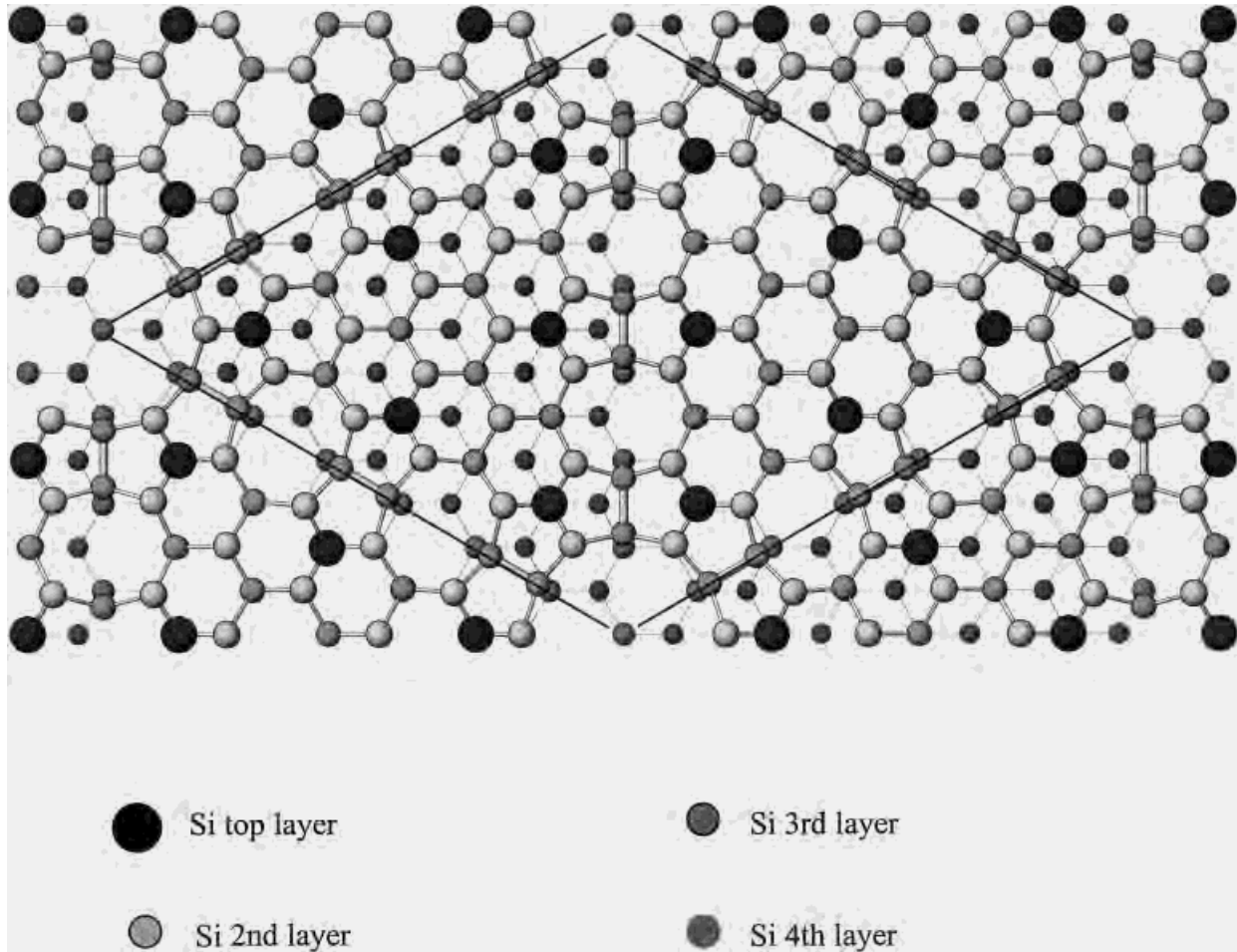


Fig. 5. Top view of the correct structure of the Si(111)-(7 × 7) surface, with the (7 × 7) unit cell outlined. Half of the fourth layer atoms lie directly under those in layers above, and so cannot be seen in this projection.

is done by means of “trial and error,” the accuracy of which depends on the quality of the initial model. Another approach is that of “direct methods” (see, for example, Giacobozzo, 1980; Schenk, 1991), in which mathematical relationships are used to derive probable phases from the observed structure factor amplitudes. Direct methods are applicable to both X-ray and electron diffraction data, and both will be considered here.

Diffraction data from surfaces are inherently problematic for direct methods (Marks and Landree, 1997), since there is usually a degree of correlation between the surface diffraction pattern, and some bulk diffraction spots. Note that the bulk spots will be many times more intense than the surface spots. Any degree of overlap between a surface and bulk diffraction spot means that the surface spot intensity cannot be measured accurately, thus leading to the possibility of either large errors in the data set, or, if many surface and bulk spots coincide, large numbers of missing reflections in the data. It should also be noted that surface diffraction patterns are inherently noisy. Finally, the exact atomic composition of a surface unit cell is rarely known, and while most direct methods are fairly tolerant of this, it should be borne in mind when analysis is carried out (Gilmore et al., 1997).

Of these problems, that of missing information is by far the most significant. In many cases, the strongest surface reflections coincide with the bulk reflections, and if these are removed, then even if all other reflections are assigned the correct phases, the holes in the data mean that the surface potential maps (for electrons-electron density maps for X-rays) will show negative areas. Even if the correct potential map is located, there is no guarantee that all of the atoms present in the structure will be found. Those that have not been displaced far from bulk positions may well be masked, leaving doubt as to their exact positions.

Despite these problems, it is possible to solve surface structures via direct methods calculations. An example of such a method that has been applied to surfaces with some success is the Maximum Entropy (ME) technique (Bricogne, 1984, 1988; Bricogne and Gilmore, 1990; Gilmore, 1996; Gilmore et al., 1990, 1993), discussed by Gilmore (1999). The method developed at Northwestern, a “Minimum Relative Entropy” (MRE) approach (Landree et al., 1997; Marks and Landree, 1997), has also proved very successful in analyzing surface structures (see Table 1), and the theoretical and practical aspects of this will be outlined below.

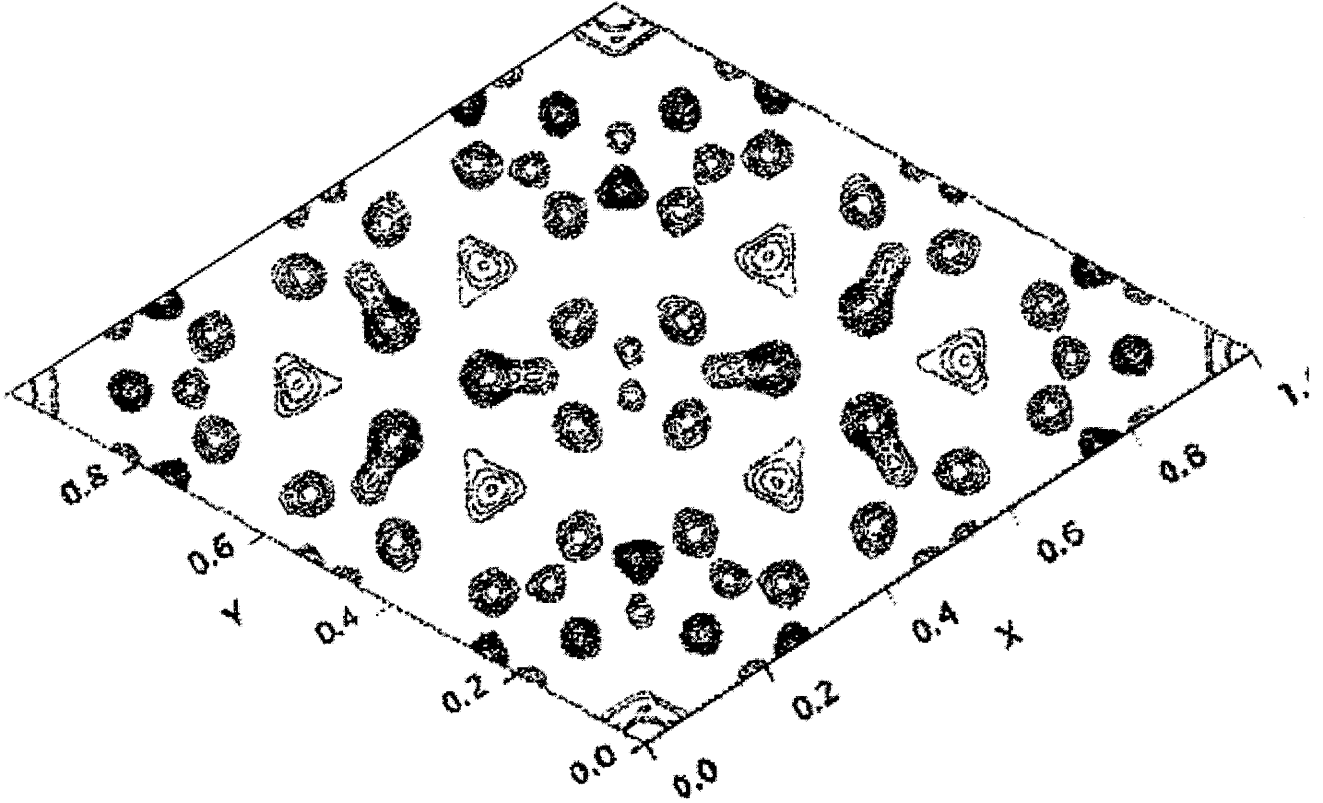


Fig. 6. Contour map showing top view of the best solution obtained by ME phase extension calculation for the Si-(111)-(7 × 7) surface, using plane group $p6mm$, showing a single (7 × 7) unit cell. Not all atoms are fully resolved.

Theory of Minimum Relative Entropy

For a complete set of unitary structure factors in reciprocal space, $\mathbf{U}(\mathbf{k})$, the Sayre equation (Sayre, 1952) states that, for non-overlapping identical atoms,

$$\mathbf{U}(\mathbf{k}) = N \sum_{\mathbf{h}} \mathbf{U}(\mathbf{k} - \mathbf{h}) \mathbf{U}(\mathbf{h}). \quad (1)$$

If some initial phases are known, the Tangent Formula (Karle and Hauptman, 1956) may be used to generate new phases, with these new phases being put back into the original equation and their validity tested by some sort of figure of merit (FOM).

This process may be considered as a Picard iteration, and equation 1 can be better represented as

$$\mathbf{U}_{n+1}(\mathbf{k}) = N \sum_{\mathbf{h}} \mathbf{U}_n(\mathbf{k} - \mathbf{h}) \mathbf{U}_n(\mathbf{h}), \quad (2)$$

where $\mathbf{U}_n(\mathbf{k})$ contains the "n"th iteration estimated phase. This may be rewritten in terms of real space, such that

$$\mathbf{u}_{n+1}(\mathbf{r}) = \hat{\mathbf{O}}[\mathbf{u}_n(\mathbf{r})], \quad (3)$$

where $\hat{\mathbf{O}}$ is some sharpening operator operating on a given real space potential map, $\mathbf{u}_n(\mathbf{r})$. The ideal opera-

tor will enhance strong features in $\mathbf{u}_n(\mathbf{r})$ while dampening weaker ones. We define the *relative entropy*, $\mathbf{S}_r(\mathbf{r})$ (Cover and Thomas, 1991) as

$$\begin{aligned} \mathbf{S}_r(\mathbf{r}) &= \mathbf{u}_n(\mathbf{r}) \ln[\mathbf{u}_n(\mathbf{r}) / \langle \mathbf{u}_n(\mathbf{r}) \rangle] \\ &+ \langle \mathbf{u}_n(\mathbf{r}) \rangle \quad \mathbf{u}_n(\mathbf{r}) > 0, \\ &= \langle \mathbf{u}_n(\mathbf{r}) \rangle \quad \mathbf{u}_n(\mathbf{r}) < 0, \end{aligned} \quad (4)$$

where $\langle \mathbf{u}_n(\mathbf{r}) \rangle$ is the mean value of $\mathbf{u}_n(\mathbf{r})$. The real space potential map, $\mathbf{u}_n(\mathbf{r})$, contains maximum information, and has maximum entropy, when $\mathbf{u}_n(\mathbf{r}) = \langle \mathbf{u}_n(\mathbf{r}) \rangle$, so as maximum information is approached, $\mathbf{S}_r(\mathbf{r}) \rightarrow 0$. Hence, the most probable solution will satisfy

$$\mathbf{u}_{n+1}(\mathbf{r}) \approx \mathbf{u}_n(\mathbf{r}) \ln[\mathbf{u}_n(\mathbf{r}) / \langle \mathbf{u}_n(\mathbf{r}) \rangle] + \langle \mathbf{u}_n(\mathbf{r}) \rangle \quad (5)$$

and, thus, the relative entropy may be used as a self-consistent sharpening operator. This operator will minimize the background present in $\mathbf{u}_n(\mathbf{r})$ while at the same time sharpening the areas that contain information.

A window function, $\mathbf{W}(\mathbf{k})$, is chosen to satisfy

$$\mathbf{w}(\mathbf{r}) = \text{FFT}[\mathbf{W}(\mathbf{k})] = \alpha \hat{\mathbf{O}}[\mathbf{w}(\mathbf{r})], \quad (6)$$

where α is some constant. This gives any single non-overlapping atom a relative entropy value of zero.

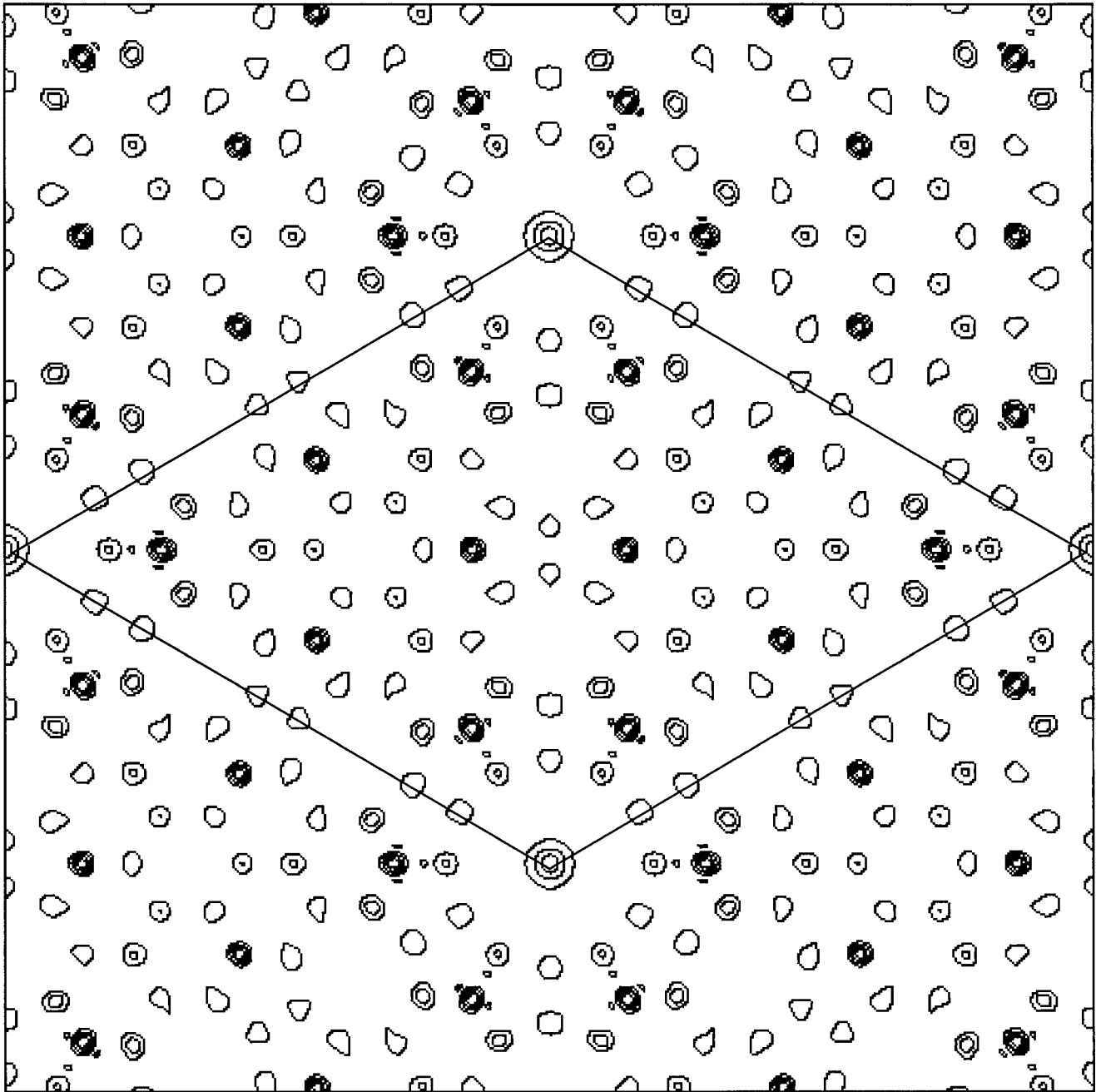


Fig. 7. Contour map showing the top view of the best solution obtained by MRE phase extension method for Si-(111)-(7 × 7) surface using plane group $p6mm$, with (7 × 7) unit cell marked. All atom positions in the first three layers are resolved.

Application of this window gives windowed unitary structure factors,

$$\mathbf{U}'(\mathbf{k}) = \mathbf{W}(\mathbf{k})\mathbf{U}(\mathbf{k}). \quad (7)$$

The \mathbf{U}' in equation 7 still satisfies equation 5, as long as a multiplicative constant for non-overlapping individual atoms is considered.

The last item required is a figure of merit (FOM), which will allow the solutions obtained to be ranked in

some way. An effective FOM is given by

$$\text{FOM} = (\sum' |\mathbf{U}_n(\mathbf{k}) - \beta \mathbf{U}_{n+1}(\mathbf{k})|) / (\sum |\mathbf{U}_n(\mathbf{k})|), \quad (8)$$

where the sum \sum' is taken over all reflections except $\mathbf{k} = \mathbf{0}$, and β is chosen to minimize the FOM.

The $\mathbf{U}_{n+1}(\mathbf{k})$ are corrected at the end of each cycle so that they have the experimentally obtained moduli. The iteration ends when the FOM stops decreasing. Thus, the lower the FOM value, the better the solution.

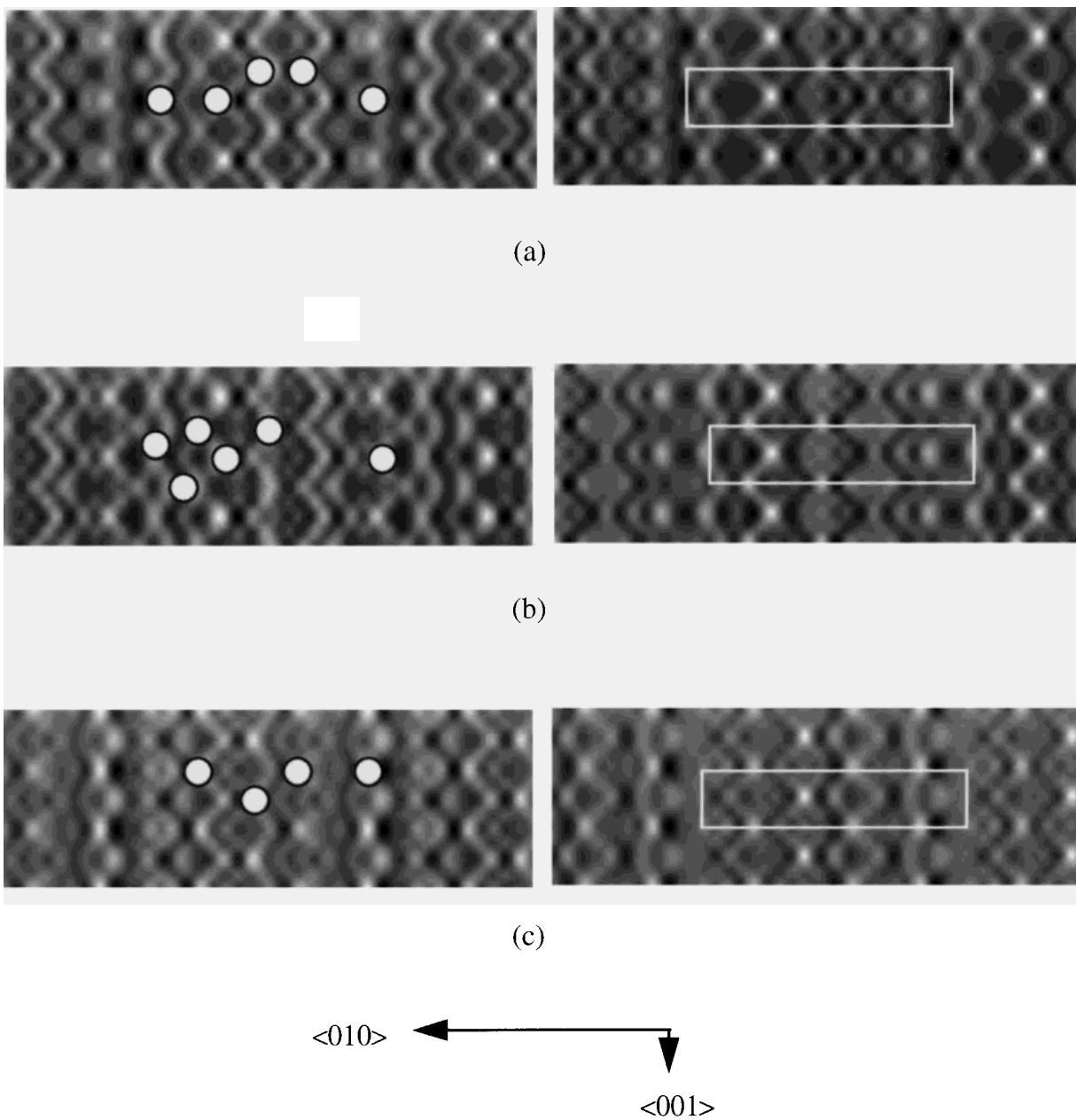


Fig. 8. Top view of best solutions obtained for TiO_2 in pm plane group with varying numbers of Ti atoms. Left-hand column shows the positions of the Ti atoms; the right-hand column shows the position of the unit cell relative to these atoms. White areas correspond to possible atom sites. **a:** 5 Ti atoms in the unit cell. **b:** 6 Ti atoms in the unit cell. **c:** 4 Ti atoms in the unit cell.

Unlike the ME method, the FOM is a measure of the consistency of the solution with the operator. In other words, if the operator changes phases and/or amplitudes dramatically, this will be reflected in a high FOM.

Genetic Algorithm

To generate the initial set of phases, and to obtain optimized solutions, a genetic algorithm is used (Chang and Lewis, 1994; Davis, 1987; Goldberg, 1989; Gutowski, 1994; Landree et al., 1997; Xiao and Williams, 1993). This starts with a set, \mathbf{S} , of structure factors. A

TABLE 2. χ^2 Values for Varying Unit Cell Contents of TiO_2 Surface

Number and type of atom in unit cell	χ^2
$4 \times \text{Ti}$	3.45
$4 \times \text{Ti}; 2 \times \text{O}$	2.27
$4 \times \text{Ti}; 3 \times \text{O}$	2.17
$4 \times \text{Ti}; 4 \times \text{O}$	2.78
$4 \times \text{Ti}; 6 \times \text{O}$	1.12
$4 \times \text{Ti}; 7 \times \text{O}$	0.937
$4 \times \text{Ti}; 8 \times \text{O}$	1.054
$4 \times \text{Ti}; 9 \times \text{O}$	0.805

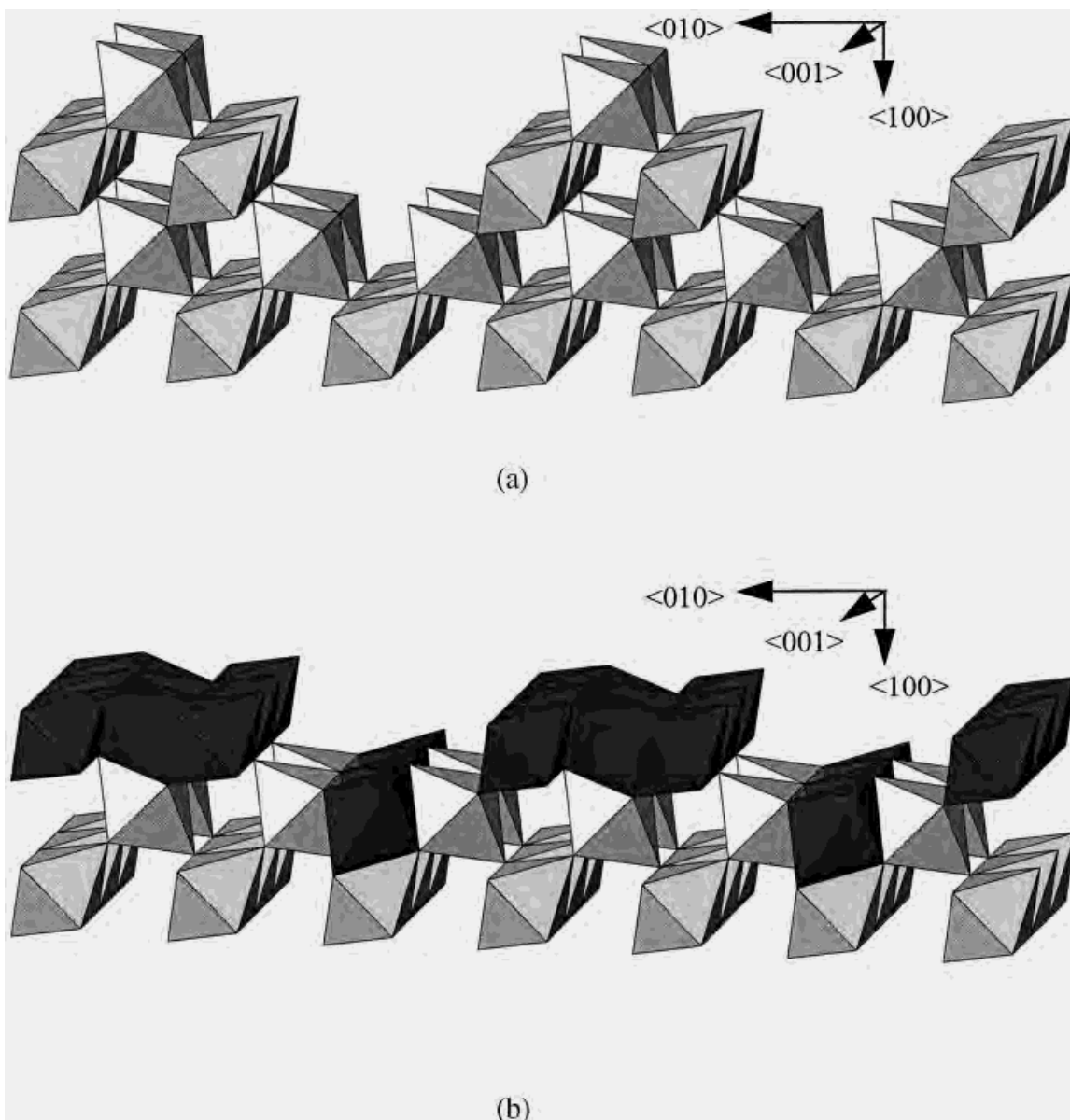


Fig. 9. **a:** Original structural model for TiO₂ (Zshack et al., 1992). **b:** Model obtained from the MRE calculation. The Ti atoms lie at the center of the octahedra, with O atoms at each corner. The new model fits the experimental data well, and is in agreement with known TiO₂ bulk structures. The dark gray octahedra show how the new model differs from the previous one.

subset of this set, \mathbf{s} , containing the strongest structure factors that have been assigned phases (see Fig. 2), is calculated. These phase values are encoded into a set of bits, which is called a *gene*. Each gene represents the phase for a single reflection, and typically between 10 and 20% of the total number of reflections present will have their phases assigned. The genes are then stored as a single string of bits, called a *chromosome*.

Starting with a *population*, \mathbf{N} , of chromosomes, the remaining phases are calculated using the MRE approach described above, and a FOM is obtained. *Natural selection* then takes place, in which *parents* are chosen for the next *generation* calculation. Parents with

low FOM values are favored. Pairs of parents produce *children* by cross-linking. This is where a location along the parent chromosomes is chosen at random, and bits on one side of this location are interchanged. Each new population thus produced is then subject to a degree of *mutation*, where bit values are randomly changed from 0 to 1, or vice versa. New phases are calculated for this population, and the FOMs obtained are evaluated as before in order to produce children for the next generation (see Fig. 2).

This relatively simple process is in fact an extremely powerful tool that is capable of global searching for minima highly efficiently. This characteristic of a genetic algorithm is attributed to the way the search

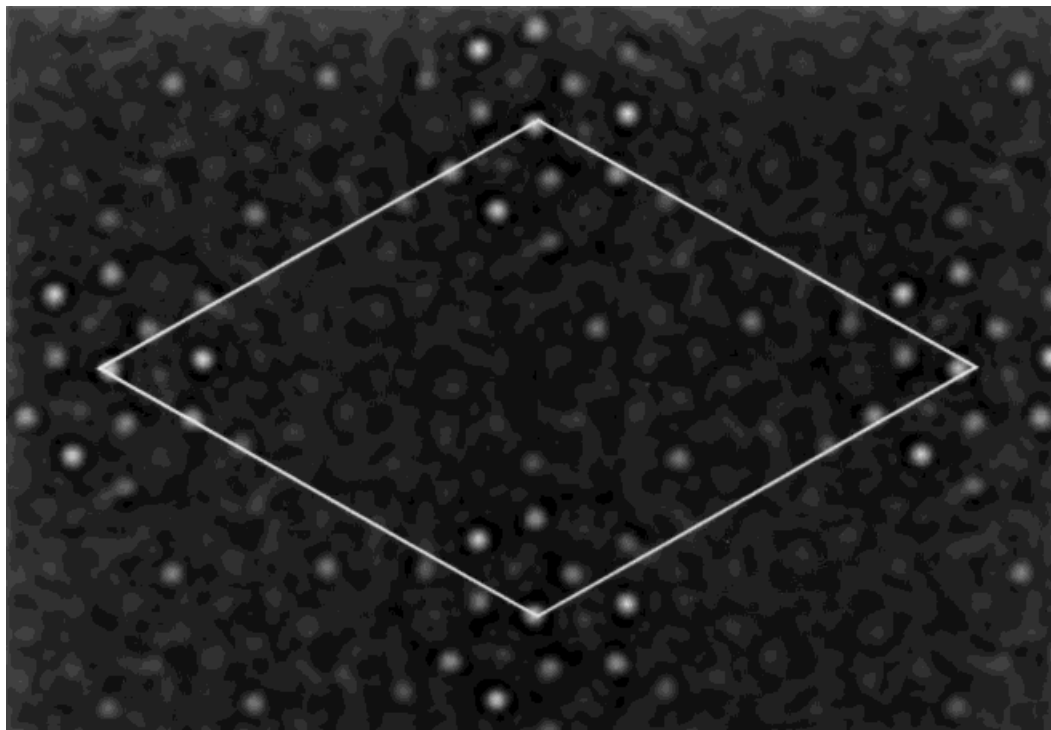


Fig. 10. The best solution obtained from the MRE analysis for the Si-(111)-(6 × 6)-Au surface, using plane group $p3$. This is a top view, with the (6 × 6) unit cell marked. White regions suggest atom positions. Not all atoms are yet resolved.

accounts for schemata. A schemata is a similarity template that describes a subset of chromosomes that have similarities at certain positions. For the simplest case, when the number of parents is equal to the number of children, the algorithm processes on the order of N^3 schemata, even though only N new FOM values are calculated for each generation. If cross-linking breaks a schemata, the search will be slowed down, so short, favorable schemata are better preserved across generations. As a schemata represents a phase choice, finding an effective schemata is akin to finding good phase choices, and thus the genetic algorithm is an excellent search engine for this type of problem.

Once solutions are obtained from the genetic algorithm search, the structure is completed for the best of these using a heavy-atom holography (Marks and Plass, 1995) algorithm that utilizes the relationship between a known wave, $\Psi(\mathbf{u})$, and an unknown wave, $\mathbf{w}(\mathbf{u})$, in the diffraction plane to determine the phase, by minimizing

$$\mathbf{P}^2 = [\mathbf{I}(\mathbf{u}) - \alpha|\Psi(\mathbf{u}) + \mathbf{w}(\mathbf{u})|^2]^2 \quad (9)$$

where $\mathbf{I}(\mathbf{u})$ is the experimental diffraction intensities of a single domain and α is the scaling factor determined by χ^2 minimization. The Fourier transform of $\mathbf{w}(\mathbf{u})$ is then an approximation of the residual wave, and atomic locations may be found by inspection of the image.

Solutions are then discriminated based upon physical or chemical considerations, and final atomic posi-

tions refined using a χ^2 minimization technique, where

$$\chi^2 = [\mathbf{1}/(\mathbf{M} - \mathbf{N})\Sigma[|\mathbf{F}_{\text{exp}}|^2 - \alpha|\mathbf{F}_{\text{calc}}|^2]^2 / \Sigma\sigma^2] \quad (10)$$

where \mathbf{M} is the number of points, \mathbf{N} the number of variables, \mathbf{F}_{exp} represents the experimentally observed amplitudes, α is a variable, \mathbf{F}_{calc} the calculated amplitudes, and σ represents the errors involved in the experiment. A χ^2 value of 1.00 represents perfect agreement between the observed and calculated structures. If a Poisson error distribution is assumed, this may be expressed as the crystallographic R-factor,

$$\mathbf{R}^n = [\mathbf{1}/(\mathbf{M} - \mathbf{N})\Sigma\||\mathbf{F}_{\text{exp}}| - \alpha|\mathbf{F}_{\text{calc}}||^n / \Sigma|\mathbf{F}_{\text{exp}}|^n] \quad (11)$$

which may also be used as a criterion for determining the “correctness” of a structure.

EXAMPLES

Thus far, the results of this method of analysis are promising. It has been able to solve both known and unknown structures for both X-ray and electron data sets. Before discussing the examples, a brief explanation of surface notation is necessary (see also Fig. 3). The most common method of surface notation allows the surface structure to be defined relative to that of the two-dimensional surface unit cell. If the surface contains an atomic arrangement identical to that of a bulk termination, it is designated (1 × 1). If, however, the surface may be represented by an arrangement of m

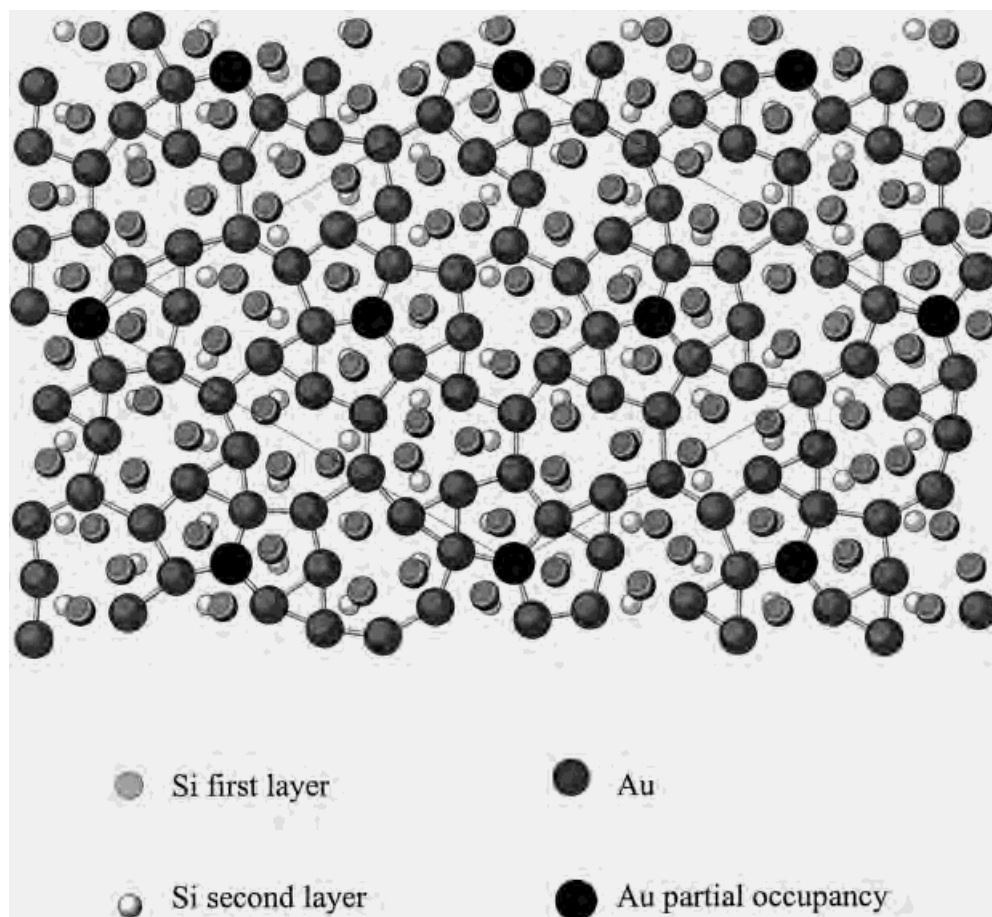


Fig. 11. Plot of atomic positions of atoms on the Si-(111)-(6 × 6)-Au surface, with (6 × 6) unit cell marked.

unit cell lengths and n unit cell widths, it is assigned ($m \times n$). In addition, the face of the surface concerned is listed, and it is usual to list the adsorbate, if one exists, so that, for example, Si (111)-(2 × 1)-Au, refers to gold on the (111) face of silicon, two surface unit cells in length and one in width.

Si (111)-(7 × 7)

The Si (111)-(7 × 7) structure has been one of the great mysteries of surface science. It proved completely unsolvable for many years, until a model was put forward in 1985 (Takayanagi et al., 1985a,b) as a result of a Patterson analysis of electron diffraction data.

This surface was analyzed via the ME technique, and also by the MRE method outlined above (Gilmore et al., 1997). One hundred and ninety-three unique diffraction reflections (Fig. 4) with resolution out to 0.6 Å were used in the analysis, and 41 phases were obtained from a high-resolution image. Despite the relatively large data set, the calculation was not straightforward due to the very strong missing reflections. The best structural-analysis results were obtained when a phase-extension calculation was carried out, using the 41 experimentally determined phases.

The top view of the correct structure is shown in Fig. 5. It should be noted that the fourth layer of atoms is complete, but half of the atoms in this layer lie directly under atoms in the layers above, and so cannot be seen

in this projection of the surface. The best solution found by means of a ME phase-extension calculation is shown in Figure 6. Notice that not all of the atoms have been found. Figure 7 shows the best solution obtained from a MRE analysis, in which all atoms in the top three layers have been resolved. Both solutions agree with the model.

TiO₂ (100)-(1 × 3)

Titanium dioxide exhibits useful catalytic properties, which have led to renewed interest in the elucidation of the surface structure of the compound (Chung et al., 1977; Munnix and Schmeits, 1984; Oliver et al., 1994). A model was proposed in 1992 (Zschack et al., 1992), based on a Patterson analysis of grazing-incidence X-ray-diffraction data. This model, though chemically feasible, agreed poorly with the experimental data.

A better solution was found using direct methods (Landree et al., 1997). The same data set of 19 unique reflections as that from which the original model was proposed was used, meaning that much information was missing, which led to problems in the refinement stage of the calculation. Four plane groups were possible, and the calculation was run for each of them. After obtaining solutions for each possible plane group, a refinement and heavy-atom holography calculation was carried out, with titanium atoms being placed at sites in the unit cells obtained. A crystallographic

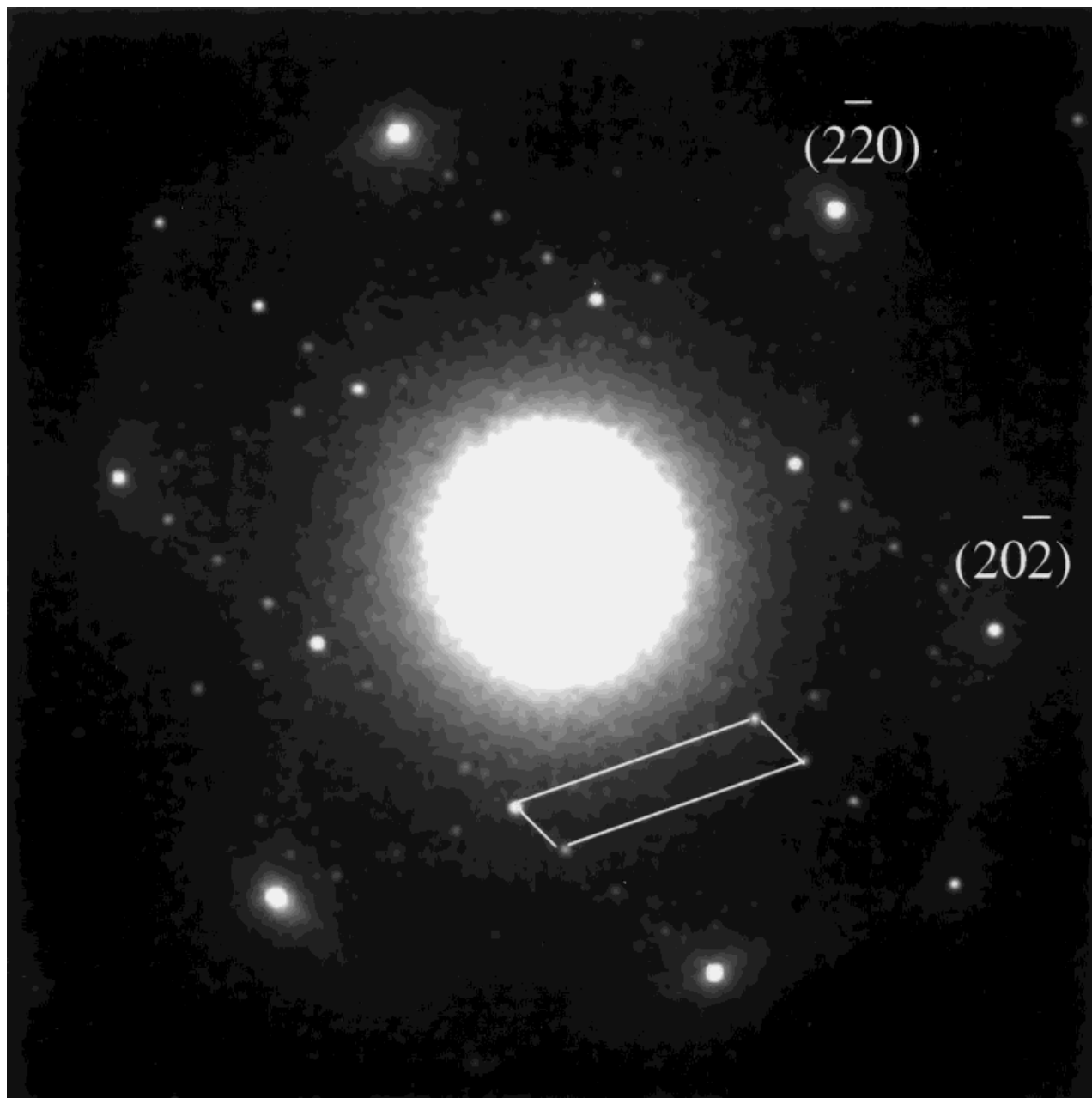


Fig. 12. TED pattern from Si-(111)-(4 × 1)-In surface. Bulk spots are indexed; (4 × 1) unit cell is marked.

R-factor calculation was carried out for each of these solutions, and only those with an R-factor of less than 0.41 were kept. All of the solutions that met this criterion fell into the same plane group, pm (Fig. 8).

Further heavy-atom holography studies showed that the best agreement between experimental and theoretical data was obtained when 4 titanium atoms and 6–8 oxygen atoms were present in the (1 × 3) unit cell (see Table 2), though with so few reflections in the data set, it is impossible to carry out a rigorous analysis for oxygen positions. Figure 9 shows a schematic of the original model and the model found by direct methods.

The model found via direct methods calculations shows non-stoichiometric features that have been documented for bulk TiO_2 , and it is reasonable to assume that this surface reconstruction reflects an ordering of these features at the surface. In addition, the new model also fits STM data.

Si (111)-(6 × 6)-Au

This surface has been studied, but the full structure was not understood (Dornisch et al., 1991). The MRE method was used with X-ray diffraction data (Marks et al., 1998a), and again the diffraction pattern suggested

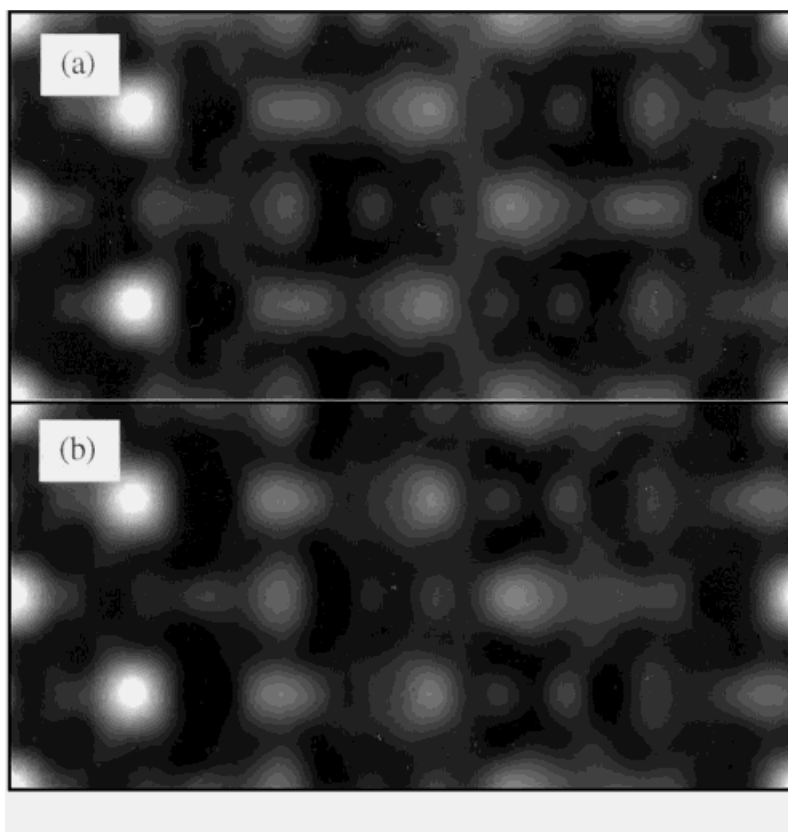
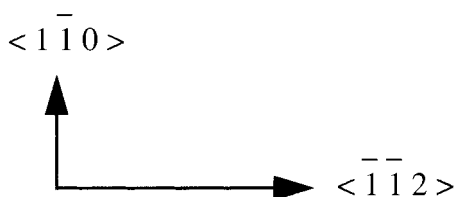


Fig. 13. Best solutions from the MRE analysis of Si-(111)-(4 × 1)-In surface. **a:** Maps that result if plane group $p2mg$ is used. **b:** Map that results if plane group pm is used. Both are two unit cells high, one unit cell wide. White areas show possible atom positions.



more than one possible plane group. Figure 10 shows one of the top maps obtained from the MRE direct method calculation, with plane group $p3$ used. As in the case of TiO_2 , heavy-atom holography was used in conjunction with an iterative refinement process to determine the full structure, which is shown in Figure 11.

Si (111)-(4 × 1)-In

This is another example of a structure that had been extensively studied but not solved (Nogami et al., 1987; Stevens et al., 1993). In particular, AES and photoemission studies suggested that four indium atoms were present in the (4 × 1) unit cell (Abukawa et al., 1995; Nakamura et al., 1991), while ion-scattering spectrometry appeared to suggest that only two indium ions were present (Cornelison et al., 1991).

Electron-diffraction data gave 27 unique reflections (Fig. 12), with four possible plane groups. The MRE calculation was run for each possibility (Collazo-Davila et al., 1997), and from the top solutions the plane groups pm and $p2mg$ were found to be the most likely (Fig. 13). After refinement and heavy-atom holography,

the final structure obtained exhibited pm symmetry, with two indium atoms in the unit cell (Fig. 14).

These examples are representative of the different types of problems that surface data present for direct methods.

DISCUSSION

Direct methods, as applied to surface structure analysis, have emerged in the last year as an exciting new tool in this important area of research. The technique still has to be fully optimized, and is perhaps less straightforward than when used for bulk structure analysis, but early difficulties, such as incomplete data, are becoming less problematic with the addition of a technique that interpolates missing reflections in a data set. Expansion of this method into three-dimensional problems has begun recently, though in the case of electron diffraction, this is limited by the difficulty in obtaining data in three dimensions. A three-dimensional approach could prove most useful in the consideration of subsurface rearrangements, since only diffraction data will give information about this. It should also be noted that, thus far, the electron data used have

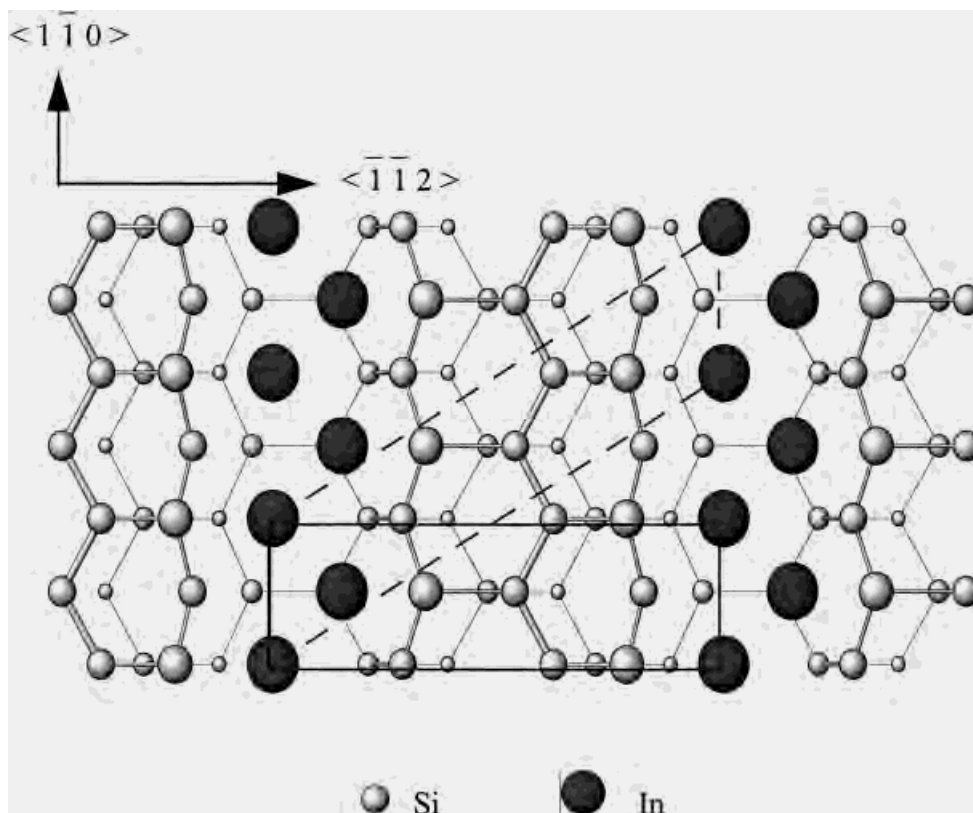


Fig. 14. Top view of atomic structure of Si-(111)-(4 × 1)-In surface. Broken line shows standard (4 × 1) unit cell; unbroken line shows the unit cell used in this analysis.

given maps of poorer quality than those produced from X-ray data, suggesting that a wholly kinematical approach to electron scattering is not completely correct.

In conclusion, direct methods for surface analysis is a specialized technique at the time of writing, and it may take some time for its advantages to be fully understood. Methods such as LEED and PEH are also extremely useful in surface structure analysis, while AES, STM, SIMS, XPS, RHEED, and RBS also prove to be of great use in providing starting points for models of surfaces. While some work is required to ensure that the data used are of good quality, there is no reason to doubt that direct methods of structure analysis will become as common a tool to the surface scientist in years to come as it is to crystallographers today.

REFERENCES

- Abukawa T, et al. 1995. Surface electronic structure of a single-domain Si(111) 4 × 1 in surface: a synchrotron radiation photoemission study. *Surf Sci* 325:33–44.
- Barker JA, Auerbach DA. 1984. Gas-surface interactions and dynamics: thermal energy atomic and molecular beam studies. *Surf Sci Rep* 4:1–99.
- Barton JJ. 1990. Photoelectron holography = holography (photoelectron diffraction). *J Elect Spectrosc Related Phenomena* 51:37–53.
- Bonevich JE, Marks LD. 1992. Ultrahigh vacuum electron microscopy of crystalline surfaces. *Microscopy* 22:95–101.
- Bricogne G. 1984. Maximum entropy and the foundations of direct methods. *Acta Cryst A* 40:410–445.
- Bricogne G. 1988. A Bayesian statistical-theory for the phase problem. 1. A multichannel maximum entropy formalism for constructing generalized joint probability-distributions of structure factors. *Acta Cryst A* 44:517–545.
- Bricogne G, Gilmore CJ. 1990. A multisolution method of phase determination by combined maximization of entropy and likelihood. 1. Theory, algorithms and strategy. *Acta Cryst A* 46:284–297.
- Chang G, Lewis M. 1994. Using genetic algorithms for solving heavy-atom sites. *Acta Cryst D* 50:667–674.
- Chu WK, Liu JR. 1996. Rutherford backscattering spectrometry: reminiscences and progresses. *Mat Chem Phys* 46:183–188.
- Chung YW, Lo WJ, Somorjai GA. 1977. Low energy electron diffraction and electron spectroscopy studies of the clean (110) and (100) titanium dioxide (Rutile) crystal surfaces. *Surf Sci* 64:588–602.
- Collazo-Davila C, et al. 1995. Design and initial performance of an ultrahigh vacuum sample preparation evaluation analysis and reaction (SPEAR) system. *J Microsc Soc Am* 1:267–279.
- Collazo-Davila C, et al. 1997. Atomic structure of the In on Si(111)(4 × 1) surface. *Surf Rev Lett* 4:65–70.
- Collazo-Davila C, et al. 1998a. Solution of Ge-(111)-(4 × 4)/Ag structure using direct methods applied to X-ray diffraction data. *Surf Sci* 418:395–406.
- Collazo-Davila C, Grozea D, Marks LD. 1998b. Determination and refinement of Ag/Si(111)-(3 × 1) surface structure. *Phys Rev Lett* 80:1678–1681.
- Cornelison DM, Worthington MS, Tsong IST. 1991. Si(111)-(4 × 1)In surface reconstruction studied by impact-collision ion-scattering spectrometry. *Phys Rev B* 43:4051–4056.
- Cover TM, Thomas JA. 1991. *Elements of information theory*. New York: John Wiley and Sons.
- Cowley JM. 1986. *Electron microscopy of surface structure*. *Prog Surf Sci* 21:209–250.
- Davis L. 1987. *Genetic algorithms and simulated annealing*. London: Pitman Publishing.
- Dornisch D, et al. 1991. Au/Si(111): Analysis of the (√3 × √3)R30° and 6 × 6 structures by In-Plane X-ray diffraction. *Phys Rev B* 44:11221–11230.
- Dorset DL. 1995. *Structural electron crystallography*. New York: Plenum Press.
- Dunn DN, et al. 1991. Preparation and detection of reconstructed plan-view surfaces. *Ultramicroscopy* 38:333–342.
- Fadley CS, et al. 1997. Diffraction and holography with photoelectrons and fluorescent X-rays. *Prog Surf Sci* 54:341–386.
- Feidenhansl R. 1989. Surface structure determination by X-ray diffraction. *Surf Sci Rep* 10:105–188.
- Giacovazzo C. 1980. *Direct methods in crystallography*. New York: Plenum Press.

- Gibson JM, Chen X, Pohland O. 1997. Transmission electron microscopy of surface and interfacial steps. *Surf Rev Lett* 4:559–566.
- Gilmore CJ. 1996. Maximum entropy and Bayesian statistics in crystallography: a review of practical applications. *Acta Cryst A* 52:561–589.
- Gilmore CJ, Bricogne G, Bannister C. 1990. A multisolution method of phase determination by combined maximization of entropy and likelihood. 2. Application to small molecules. *Acta Cryst A* 46:297–308.
- Gilmore CJ, Shankland K, Bricogne G. 1993. Applications of the maximum entropy method to powder diffraction and electron crystallography. *Proc R Soc Lond A* 442:97–111.
- Gilmore CJ, et al. 1997. Direct solutions of the Si(111)(7 × 7) structure. *Surf Sci* 381:77–91.
- Gilmore CJ. 1999. Maximum entropy methods in electron crystallography. *Microsc Res Tech* 46:117–129.
- Goldberg DE. 1989. Genetic algorithms in search, optimization and machine language. Reading, MA: Addison-Wesley Publishing Company Inc.
- Greenlief CM, White JM. 1993. Secondary ion mass spectroscopy. In: Rossiter BW, Baetzold RC, editors. Investigations of surfaces and interfaces, part A. Physical methods of chemistry, vol 9A, 2nd ed. New York: John Wiley and Sons; p 321–381.
- Grimblot J, Gengembre L, Dhuysser A. 1990. XPS: a routine technique to characterize surfaces of practical catalysts. *J Electr Spectrosc Related Phenomena* 52:485–509.
- Grozea D, et al. 1998. Structural investigations of metal-semiconductor surfaces. *Micron* 30:41–49.
- Gutowski MW. 1994. Smooth genetic algorithm. *J Phys A* 27:7893–7904.
- Hashizume T, et al. 1994. Structures of As-rich GaAs (001)-(2 × 4) reconstruction. *Phys Rev Lett* 73:2208–2211.
- Hashizume T, et al. 1995. Determination of the surface structures of the GaAs (001)-(2 × 4) As-rich phase. *Phys Rev B* 51:4200–4212.
- Hauptman H, Karle J. 1953. Solution of the phase problem. I. The centrosymmetric crystal. A. C. A. Monograph No. 3. Pittsburgh: Polycrystal Book Service.
- Heinz K. 1988. Structural analysis of surfaces by LEED. *Prog Surf Sci* 27:239–326.
- Heinz K. 1994. Diffuse LEED and local surface structure. *Phys Stat Sol* 146:195–204.
- Heinz K. 1995. LEED and DLEED as modern tools for quantitative surface structure determination. *Rep Prog Phys* 58:637–704.
- Hudson JB. 1992. Surface science: an introduction. Boston: Butterworth-Heinemann.
- Ichimiya A, et al. 1993. Theory of RHEED and application to surface structure studies. *Ultramicroscopy* 48:425–432.
- Ichimiya A, Ohno Y, Horio Y. 1997. Structural analysis of crystal surfaces by reflection high energy electron diffraction. *Surf Rev Lett* 4:501–511.
- Ikarashi N, et al. 1988. Profile and plan-view imaging of reconstructed surface structures of gold. *Ultramicroscopy* 26:195–203.
- Jayaram G, Xu P, Marks LD. 1993. Structure of Si (100)-(2 × 1) surface using UHV transmission electron diffraction. *Interface Sci* 2:379–395.
- Jayaram G, Plass R, Marks LD. 1995. UHV-HREM and diffraction of surfaces. *Interface Sci* 2:379–395.
- Jona F, Strozier JA, Yang W. 1982. Low-energy electron-diffraction for surface structure analysis. *Rep Prog Phys* 45:527–585.
- Karle J, Hauptman H. 1956. A theory of phase determination for the four types of non-centrosymmetric space groups 1P222₁, 2P22, 3P₁2, 3P₂2. *Acta Cryst* 9:635–651.
- Korte U, Meyerehmsen G. 1993. Dynamical RHEED from disordered surfaces: sharp reflections and diffuse scattering. *Surf Sci* 298:299–306.
- Landree E, Collazo-Davila C, Marks LD. 1997. A multi-solution genetic algorithm approach to surface structure determination using direct methods. *Acta Cryst B* 53:1677–1680.
- Landree E, et al. 1998. Structure of the TiO₂(100)-1 × 3 surface by direct methods. *Surf Sci* 408:300–309.
- Len PM, et al. 1995. Photoelectron holography: prospects and limitations of direct methods. *J Electr Spectrosc Related Phenomena* 76:351–357.
- Ma Y, Marks LD. 1990. Surface phenomena in RHEED and REM. *Acta Cryst A* 46:594–606.
- Ma Y, Marks LD. 1992. Developments in the dynamic theory of high-energy electron reflection. *Microsc Res Tech* 20:371–389.
- Maksym PA. 1985. Analysis of the intensity data for RHEED by the MgO (001) surface. *Surf Sci* 149:157–174.
- Maksym PA, Beeby JL. 1981. A theory of RHEED. *Surf Sci* 110:423–438.
- Marks LD. 1983. Direct imaging of carbon-coated and clean gold (110) surfaces. *Phys Rev Lett* 51:1000–1002.
- Marks LD. 1984. Direct imaging of solid surfaces. I: image simulation and interpretation. *Surf Sci* 139:281–298.
- Marks LD. 1992a. Registry and UHV transmission electron diffraction of surfaces. *Ultramicroscopy* 45:145–154.
- Marks LD. 1992b. Atomic scale imaging of surfaces in UHV. In: Bailey GN, Bentley J, Small JA, editors. Proc. 50th EMSA. San Francisco: San Francisco Press. p 290–291.
- Marks LD, Landree E. 1997. A minimum entropy algorithm for surface phasing problems. *Acta Cryst A* 54:.
- Marks LD, Plass R. 1995. Atomic structure of Si(111)-(5 × 2)-Au from high resolution electron microscopy and heavy-atom holography. *Phys Rev Lett* 75:2172–2175.
- Marks LD, Smith DJ. 1983. Direct surface imaging in small metal particles. *Nature* 303:316–317.
- Marks LD, et al. 1991. UHV microscopy of surfaces. *Ultramicroscopy* 27:90–102.
- Marks LD, et al. 1992. Atomic imaging of surfaces in plan view. *EMSA Bull* 22:65–69.
- Marks LD, Xu P, Dunn D. 1993. UHV transmission electron microscopy of Ir (001). 2. Atomic positions of the (5 × 1) reconstructed surface from HREM and R-factor refinements. *Surf Sci* 294:322–332.
- Marks LD, et al. 1998a. Au 6 × 6 on Si (111): evidence for a 2-D pseudo glass. *Surf Rev Lett* 5:459–464.
- Marks LD, Plass R, Dorset DL. 1997. Imaging surface structures by direct phasing. *Surf Rev Lett* 4:1–8.
- Marks LD, et al. 1998. Direct methods for surfaces. *Surf Rev Lett*.
- Mitura Z, Maksym PA. 1993. Analysis of reflection high-energy electron diffraction azimuthal plots. *Phys Rev Lett* 70:2904–2907.
- Mroz S. 1996. Studies of composition of surfaces and interfaces with the use of Auger electron spectroscopy. *Acta Phys Pol A* 89:183–193.
- Munnix S, Schmeits M. 1984. Electronic structure of ideal TiO₂(110), TiO₂(001) and TiO₂(100) surfaces. *Phys Rev B* 30:2202–2211.
- Nakahara H, Ichimiya A. 1991. Structural study of Si growth on a Si (111) 7 × 7 surface. *Surf Sci* 241:124–134.
- Nakamura N, Anno K, Kono S. 1991. Surface analysis of the single-domain Si(111) 4 × 1-In surface by μ-probe Auger electron diffraction and μ-probe reflection high-energy electron diffraction. *Surf Sci* 256:129–134.
- Nihoul G, Abdelmoula K, Métois JJ. 1984. High resolution images of a reconstructed surface structure on (111) gold platelets: interpretation and comparison with theoretical models. *Ultramicroscopy* 12:353–366.
- Nogami J, Sang-il Park, Quate CF. 1987. Indium-induced reconstructions of the Si(111) surface studied by scanning tunneling microscopy. *Phys Rev B* 36:6221–6224.
- Oliver PM, et al. 1994. Atomistic simulations and electronic structure of TiO₂ (100) surfaces. *Surf Sci* 307–309:1200–1205.
- Pendry JB. 1974. Low energy electron diffraction. London: Academic Press.
- Pendry JB. 1994. Multiple scattering theory of electron diffraction. *Surf Sci* 299/300:375–390.
- Pendry JB, Saldin DK. 1984. SEXAFS without X-rays. *Surf Sci* 145:33–47.
- Peng LM, Cowley JM. 1986. Dynamical diffraction calculations for RHEED and REM. *Acta Cryst A* 42:545–552.
- Peng LM, Dudarev SL, Whelan MJ. 1996. Approximate methods in dynamical RHEED calculations. *Acta Cryst A* 52:909–922.
- Plass R, et al. 1998. Cyclic ozone identification in magnesium oxide (111) surface reconstructions. *Phys Rev Lett*. 81:4891–4894.
- Price GL. 1992. In: O'Connor DJ, Sexton BA, Smart RSC, editors. Surface analysis methods in materials science, Springer Series in Surface Science, vol. 23. Berlin: Springer-Verlag. p 263–274.
- Pruett M. 1994. Introduction to surface physics. Oxford: Clarendon Press. p 5–6.
- Reuter K, et al. 1997. Holographic image reconstruction from electron diffraction intensities of ordered superstructures. *Phys Rev Lett* 79:4818–4821.
- Robinson IK, Tweet DJ. 1992. Surface X-ray diffraction. *Rep Prog Phys* 55:599–651.
- Rous PJ. 1992. The Tensor LEED approximation and surface crystallography by low-energy electron diffraction. *Prog Surf Sci* 39:3–63.
- Rous PJ, Pendry JB. 1989a. The theory of tensor LEED. *Surf Sci* 219:355–372.
- Rous PJ, Pendry JB. 1989b. Applications of tensor LEED. *Surf Sci* 219:373–394.
- Rous PJ, et al. 1986. Tensor LEED: a technique for high-speed surface-structure determination. *Phys Rev Lett* 57:2951–2954.

- Rous PJ, Van Hove MA, Somorjai GA. 1990. Directed search methods for surface structure determination by LEED. *Surf Sci* 226:15–25.
- Saldin DK. 1997. Holographic crystallography for surface studies: a review of the basic principles. *Surf Rev Lett* 4:441–458.
- Saldin DK, De Andres PL. 1990. Holographic LEED. *Phys Rev Lett* 64:1270–1273.
- Sayre D. 1952. The squaring method: a new method for phase determination. *Acta Cryst* 5:60–65.
- Schenk H, editor. 1991. *Direct methods of solving crystal structures*. New York: Plenum Press.
- Somorjai GA. 1995. *Introduction to surface chemistry and catalysis*. New York: John Wiley and Sons. p 12–13.
- Somorjai GA, Starke U. 1992. Monolayer surface structure analysis. *Pure Appl Chem* 64:509–527.
- Spence JHC, Weierstall U, Lo W. 1996. Atomic species identification in scanning tunneling microscopy by time of flight spectroscopy. *J Vac Sci Technol B* 14:1587–1590.
- Stevens JL, Worthington MS, Tsong IST. 1993. 4×1 Reconstruction of indium deposited on vicinal Si(111) surfaces. *Phys Rev B* 47:1453–1459.
- Szöke A. 1986. X-ray and electron holography using a local reference beam. In: Attwood DT, Bokor J, editors. *Short wavelength coherent radiation: generation and applications*. New York: American Institute of Physics; p 361–367.
- Takayanagi K, et al. 1978. Techniques for routine UHV *in situ* electron microscopy of growth processes of epitaxial thin films. *J Phys E* 11:441–448.
- Takayanagi K, et al. 1985a. Structural analysis of Si(111)- 7×7 by UHV transmission electron diffraction and microscopy. *J Vac Sci Technol A* 3:1502–1506.
- Takayanagi K, et al. 1985b. Structure analysis of Si(111)- 7×7 reconstructed surface by transmission electron diffraction. *Surf Sci* 164:367–392.
- Tanishiro Y, Takayanagi K. 1989. Validity of the kinematical approximation in transmission electron diffraction for the analysis of surface structures. *Ultramicroscopy* 27:1–8.
- Tong SY. 1994. Electron diffraction for surface studies: the first 30 years. *Surf Sci* 299/300:358–374.
- Turner NH, Schreifels JA. 1994. Surface analysis: X-ray photoelectron spectroscopy and Auger electron spectroscopy. *Anal Chem* 66:R163–R185.
- Twisten RD, Gibson JM. 1994. Kinematic analysis of transmission electron diffraction data from Si(111)- 7×7 . *Ultramicroscopy* 53:223–235.
- Vainshtein BK. 1964. *Structure analysis by electron diffraction*. Oxford: Pergamon Press.
- van de Leemput LEC, van Kempen H. 1992. Scanning tunneling microscopy. *Rep Prog Phys* 55:165–240.
- Van Hove MA. 1997. Determination of complex surface structures with LEED. *Surf Rev Lett* 4:479–487.
- Venables JA, Spiller GDT, Hanbucken M. 1984. Nucleation and growth of thin films. *Rep Prog Phys* 47:399–459.
- Wander A, Pendry JB, Van Hove MA. 1992. Linear approximation to dynamical low-energy electron diffraction. *Phys Rev B* 46:9897–9899.
- Wei CM, Tong SY. 1992. Direct atomic structure by holographic diffuse LEED. *Surf Sci Lett* 274:L577–L582.
- Weissmann R, Müller K. 1981. Auger electron spectroscopy: a local probe for surfaces. *Surf Sci Rep* 1:251–309.
- Williams ED, Marks LD. 1995. New and emerging techniques for imaging surfaces. *Crit Rev Surf Chem* 5:275–303.
- Woolfson MM, Fan H-F. 1995. *Physical and non-physical methods of solving crystal structures*. Cambridge: Cambridge University Press.
- Xiao YL, Williams DE. 1993. Genetic algorithm: a new approach to the prediction of the structure of molecular structures. *Chem Phys Lett* 215:17–24.
- Xu P, Marks LD. 1992a. Intensity measurement of surface diffraction spots by EELS. In: Bailey GW, Bentley J, Small JA, editors. *Proc. 50th EMSA, San Francisco*: San Francisco Press. p 282–283.
- Xu P, Marks LD. 1992b. Intensities of surface diffraction spots in plan view. *Ultramicroscopy* 45:155–157.
- Xu P, Jayaram G, Marks LD. 1994. Cross-correlation method for intensity measurement of transmission electron diffraction patterns. *Ultramicroscopy* 53:15–18.
- Zangwill A. 1988. *Physics at surfaces*. Cambridge: Cambridge University Press.
- Zschack P, Cohen JB, Chung YW. 1992. Structure of the TiO₂-(100)-(1 × 3) surface determined by glancing angle X-Ray diffraction and low-energy electron-diffraction. *Surf Sci* 262:395–408.